Asian Journal of Water, Environment and Pollution, Vol. 18, No. 4 (2021), pp. 109–118.
DOI 10.3233/AJW210050

Mitigating Water Pollution Using a Sustainable Biobased Low-Cost Adsorbent Derived From Mustard Straw

Kalpana Patidar, Manish Vashishtha*, Sonal Rajoria and Tarun Kumar Chaturvedi

Department of Chemical Engineering, Malaviya National Institute of Technology, Jaipur, Rajasthan – 302017, India
✉ mvashishtha.chem@mnit.ac.in

Received September 15, 2021; revised and accepted September 21, 2021

Abstract: The present work is focussed on treating dye-laden polluted water by using a mustard straw-based activated carbon prepared using $ZnCl_2$ and H_3PO_4 activation methods. The activation conditions based on the parameters reported in the literature are taken as follows: 700 °C activation temperature, impregnation ratio 2.0, and heating time 2 h. The textural and surface properties of mustard stalk activated carbon (MSAC) were studied by using SEM, nitrogen adsorption, and FT-IR, whereas its adsorption capacity was obtained using the methylene blue (MB) adsorption method. Activation of $ZnCl_2$ and H_3PO_4 resulted in a BET surface area of 402 and 496 m^2/g, respectively. The average pore diameter of the MSAC was found to be 2.13 and 2.59 nm for $ZnCl_2$ and H_3PO_4 activation respectively. The Langmuir and Freundlich models were applied to evaluate the equilibrium parameters of MB adsorption. The monolayer adsorption capacity of MSAC by $ZnCl_2$ and H_3PO_4 for MB removal from the Langmuir model were 122.25 and 213.21 mg/g respectively. Activation with H_3PO_4 was found to be more effective in modifying the structure of the mustard straw when compared with $ZnCl_2$ and also it resulted in a higher adsorption capacity of MB. The present work highlights that the MSAC produced using H_3PO_4 activation is a low-cost bio-based adsorbent using abundant agricultural by-product namely mustard straw, and this adsorbent can be used in numerous industrially important applications.

Key words: Mustard straw, adsorption, H_3PO_4, $ZnCl_2$, isotherm.

Introduction

Biomass-based activated carbon can be used to remove pollutants and adsorption of dyes from wastewater. Many dyestuffs and chemicals are used after mixing with water in various processes in the textile, leather, paper and pulp industry, tannery, and paint industries (Siddiqui et al., 2019). Once processes are complete, leftover dye effluent is discarded without further treatment into the water bodies and environment. This wastewater is toxic and causes harmful effects on animals and human health (Talaiekhozani et al., 2020). Various physical, chemical, and biological treatments are available to treat the effluent that comes out from these industries. Among these processes adsorption is one of the most efficient processes for remediation of dye effluent due to its ease of operations, cost-effectiveness, environmentally friendly, and high efficiency. A large number of studies are based on various types of biobased adsorbents for wastewater treatment (Siddiqui, et al., 2019); however, no significant study is available on utilising mustard crop residue for making adsorbent for industrial applications. The current study is aimed at filling this research gap in which the removal of methylene blue (MB) dye from water using activated carbon derived from mustard straw biomass using $ZnCl_2$ and H_3PO_4 activators is studied. MB is a cationic dye

*Corresponding Author

that is used in textile (colour wool, cotton, and leather), paper and paint industries (Pandey, 2019).

India is predominantly an agrarian economy. After harvesting and processing of any agricultural crop taking out its productive yield a large amount of leftover waste in terms of stalk, straw, husk, etc (Gonzalez-Garcia, 2018) is generated. Out of this waste, a large amount is used either in firewood or is burned on-farm primarily to clear the field from straw and stubble of the preceding crop so that succeeding crops can be properly sown (Hama et al., 2020). The burning of crop residues leads to the release of particulate matter, emission of greenhouse gases, and smoke causing human health problems, in turn, global warming; loss of plant nutrients, and atmospheric pollution (Gogoi et al., 2017). Therefore, these agricultural waste or residues must be turned into valuable and economically viable products to meet dual targets of increasing farm income and reducing the disposal problem of agricultural waste also called biomass waste (Liu et al., 2016). Many researchers have explained strategies to utilise agricultural waste in different ways like making composite materials, preparation of biochar, and production of activated carbon, etc (Bulgariuet al., 2019; Fang, 2012; Sangonet al., 2018). Activated carbon (AC) is a carbonaceous material characterised by a high surface area, high porosity, and good adsorption capacity thereby making it a promising material for its use in varied applications like wastewater treatment, gas storage, fuel cell, and adsorption, etc (Reffas et al., 2010). AC is derived by using physical and chemical activation methods. The chemical activation is done using activators like KOH, H_3PO_4, $ZnCl_2$, NaOH, K_2CO_3, etc at high temperatures, whereas physical activation is carried out at high temperatures in steam or air atmosphere (Jawad et al., 2018; Liu et al., 2018). Out of the two activation routes, chemical activation is achieved in a shorter time with low energy consumption. Commercially available AC derived from coal and biomass like coconut shell have high cost, therefore it becomes imperative to reduce the cost of preparation to meet the demand of AC, and with this aim, many researchers are trying to produce low-cost AC based on abundantly available lignocellulosic biomass materials.

In the present work, one such agro residue or biomass waste, namely mustard crop residue, is chosen for study since mustard is one of the largest consumed oilseeds globally and consequently, it also generates a large amount of agro residue. The worldwide production of mustard is 68.19 million metric tons per year (MMt/y) and the Canada, European Union, China, and India are its leading producers (2019-2020 data) (https://www.statista.com). India contributes about 7.7 MMt/y of the worldwide generation. Processing of one metric ton of mustard seed generates 1.85 tons of agro residue in the form of a mustard stalk and straw (Purohit et al., 2007). Since mustard crop residue is not even fit for animal consumption as fodder, due to its glucosinolate content, so a proper waste management strategy is needed to efficiently utilise it. Mustard crop residue is highly renewable and sustainable biomass, containing cellulose (48.3%), hemicellulose (29.56%), and lignin (24.56%) on a weight basis (Singh et al., 2013). Mustard straw activated carbon (MSAC) was prepared and characterised using SEM, FTIR, and BET surface area. Isotherm studies were also performed.

Materials and Experimental Methods

Materials and Reagents

Mustard straw (MS) was procured from a locally available village near Jagatpura, Jaipur (Rajasthan), India. It was first washed several times with water to remove adhering impurities and that washed sample was dried under an air dryer oven overnight at 105 °C. Dried MS was ground to powder by using a laboratory ball mill and sieved to 60-80 µm particle size, which was used as a precursor. In the present study, $ZnCl_2$ and H_3PO_4 were used as an activating agent, which was purchased from MERK, India. Methylene blue ($C_{16}H_{18}ClN_3S$ and molecular weight is 319.85 g/mol) was used as adsorbate also obtained from MERK, India.

Preparation of Activated Carbon

Dried MS was first carbonised at 650 °C and maintained for 1.5 h under a nitrogen environment to obtain biochar. Thereafter, the resultant biochar was collected and stored in a desiccator for further use. The post-activation process was performed by mixing the biochar with $ZnCl_2$ and H_3PO_4 solutions (impregnation ratio 2.0) at 80 °C for 6 h and followed by removing water from the solution by keeping it under an oven at 105 °C. About 4 g impregnated dried mixture was taken for activation process in a tubular furnace at 700 °C for an hour under nitrogen atmosphere. The resulted sample obtained from the activation process is taken out from the furnace and washed with HCl and hot and cold distilled water until pH was maintained to 7. The samples were designated as AC-$ZnCl_2$ (using $ZnCl_2$ as activating agent) and AC-H_3PO_4 (using H_3PO_4 as activating agent).

Sample Characterisation

The morphological and elemental studies of MSAC are analysed by using scanning electron microscopy (SEM) with Energy Dispersive X-ray (EDX) (NOVA nano FE-SEM 450, FE). Fourier Transformer Infrared (FTIR) (FT-IR Spectrum 2, Perkin Elmer) is used to analyse the functional groups, chemical bonds, and chemical compounds present in a sample. In the present study, potassium bromide (KBr) is used as a reference with a working spectra range of 4000 to 400 cm^{-1}. Nitrogen adsorption/desorption experiments were conducted using Quantachrome Autosorb Analyzer (using N_2 at 77 K). The total pore volume determination was performed under nitrogen adsorption process and the value obtained was $p/p_0 = 0.98$.

Experimental Protocol and Isotherm Study

The batch study of MB adsorption on AC-$ZnCl_2$ and AC-H_3PO_4 were run in a set of 250 mL flask containing 100 mL solution of MB at various adsorption dosages with different initial concentrations. Solutions were agitated by shaker run at 120 rpm at 30 °C and followed by decantation using centrifuge and filtration. The equilibrium concentration of solutions is analysed using a UV-visible spectrophotometer at 664 nm. The adsorption capacity (mg/g) and percentage removal of MB are obtained by using Equations (1) and (2).

$$q_e = \frac{C_o - C_e}{m} V \tag{1}$$

$$R = \frac{C_o - C_e}{C_o} 100 \tag{2}$$

here,

C_o is initial concentration and C_e is equilibrium concentrations of MB dye solution in mg/L respectively, V is the volume of dye solution in L, m is the mass of dry AC (adsorbent) in g used.

Langmuir and Freundlich isotherm models (; Freundlich, 1906; Langmuir, 1916) were used to understand the relationship between the distribution of adsorbed dye molecules and their equilibrium concentrations explained by the following equations :

Langmuir isotherm: $$\frac{C_e}{q_e} = \frac{1}{q_m K} + \frac{C_e}{q_m} \tag{3}$$

$$R_L = \frac{1}{(1 + KC_o)} \tag{4}$$

Freundlich isotherm: $$\ln q_e = \ln K_f + \frac{1}{n} \ln C_e \tag{5}$$

where,

q_e is the adsorbed capacity of MB dye at the equilibrium in mg/g,

C_o and C_e is initial and equilibrium solute concentration in mg/L,

q_m is the maximum adsorption capacity corresponding to complete monolayer coverage in mg/g,

R_L value implies the favourable adsorption process at a temperature range from 30-50 ^oC,

K is the Langmuir constant related to the energy of the adsorption in L/mg and

K_f and *1/n* are the empirical constants dependent on the nature of adsorbent and adsorbate.

Results

SEM with EDX Analysis

Figure 1 shows the SEM microstructure of biochar and MSAC (AC-$ZnCl_2$ and AC-H_3PO_4). Figure 1a shows irregular and longitudinal fibres of the biochar of MS, which are visible, however, after carbonisation, the AC samples show pores and honeycomb structures with some degree of porosity (Figure 1 b,c). Due to its amorphous structure, AC is useful for the removal of MB on MSAC. EDX and BET analyses of samples are shown in Table 1. In BET analysis, the diameter of particles is classified based on size ranges *viz.* micro (0-2 nm), meso (2-50 nm), and macro (50-7500 nm) according to IUPAC. The specific BET surface area of MS-biochar is found to be 95 m^2/g, it increased after the activation process to 402 and 496 m^2/g for $ZnCl_2$ and H_3PO_4 activation, respectively. Table 1 shows that the average diameter of activated carbon was more than 2 nm which means AC-$ZnCl_2$ and AC-H_3PO_4 possess mesopores properties.

FTIR Analysis

Figure 2 shows an analysis of surface functionality of activated carbon before and after MB was loaded for adsorption using the FTIR method. It can be seen that in Figure 2 a,b that all stretching peaks occur within a range of 3550-3200 cm^{-1} ascribed to the hydroxyl group (alcohol, carboxylic acids, and phenols) present on the adsorbent surface as listed in Table 2. Figure 2 also shows that vibrational peaks of activated carbon are shifted towards high adsorption peaks in MB-loaded activated carbon. The vibrational bands at the range of 3000-2800, 2140-1990, 1670-1300, 1250-1030, and 1000-650 cm^{-1} can be attributed to N-H, N=C=S, C=C, N-H, N-O, C-H, C-N functional group appear in the adsorbent. However, after adsorption of MB dye onto the activated carbon (AC-$ZnCl_2$ and AC- H_3PO_4) some additional stretching bands of AC-$ZnCl_2$ (2067.85, 1465.5 cm^{-1}) and AC- H_3PO_4 (2073.22, 1371 cm^{-1})

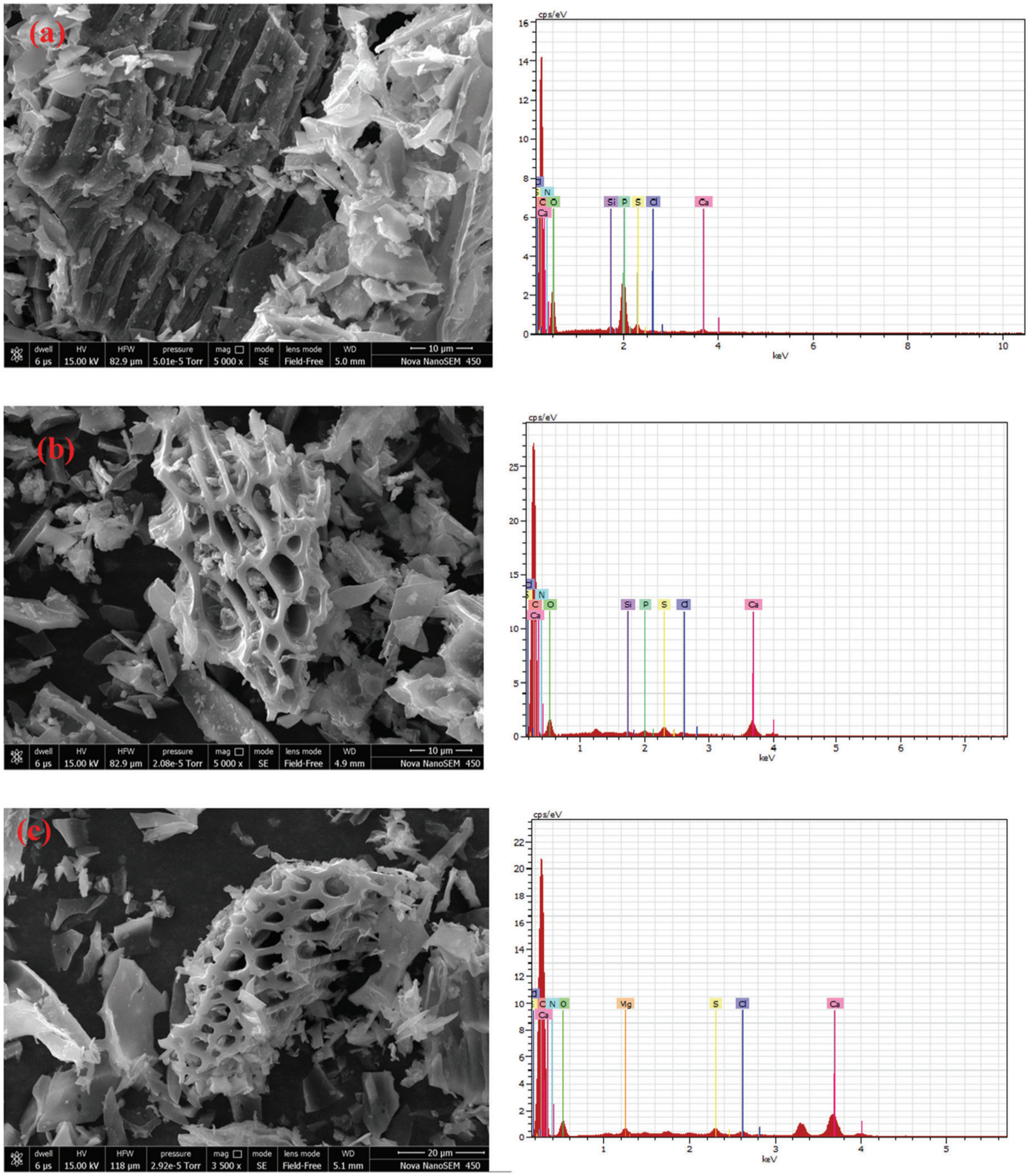

Figure 1: The SEM image of (a) biochar, (b) Ac-$ZnCl_2$, and (c) AC-H_3PO_4.

due to N-O, N=C=S, C-N functionality characteristics are seen.

Adsorption and Isotherm Study

Effect of Adsorption Dosage

To obtain the isotherm study for adsorption of MB using AC-$ZnCl_2$ and AC-H_3PO_4, the present study was initially aimed at understanding the effect of dosages of AC on the adsorption of MB. Figure 3 depicts the effect of dosages of adsorbent on 25 mg/L MB solution. The adsorbent doses were varied from 50 to 500 mg/L. It can be seen from Figure 3 that the removal of MB by both the AC sharply increased from 50 to 300 mg/L due to the availability of more specific surface area and adsorbent sites of AC. Thereafter, beyond 350 mg/L and 200 mg/L of AC-$ZnCl_2$ and AC-H_3PO_4 respectively, no significant increase in the removal efficiency of MB was observed, this can be due to the decrease in free

Table 1: Elemental and BET analysis of biochar and activated carbon

Property	*Biochar*	*AC-$ZnCl_2$*	*AC-H_3PO_4*
Ultimate analysis			
C, wt. %	72.07	80.84	77.13
O, wt. %	23.97	15.88	13.70
N, wt. %	2.95	0.08	2.23
P, wt. %	-	0.12	3.43
S, wt. %	0.40	0.48	0.33
Ca, wt. %	0.34	2.38	2.83
Si, wt. %	0.24	0.04	0.06
Cl, wt. %	0.02	0.18	0.29
Surface Property (BET analysis)			
Bulk density, kg/m^3	86 (unprocessed)	503.23	501.60
Average pore diameter, nm	-	2.13	2.59
BET surface area, m^2/g	95	402	496
Total pore volume, cm^3/g	0.081	0.33	0.34
Mesoporous volume, cm^3/g	0.06	0.17	0.18

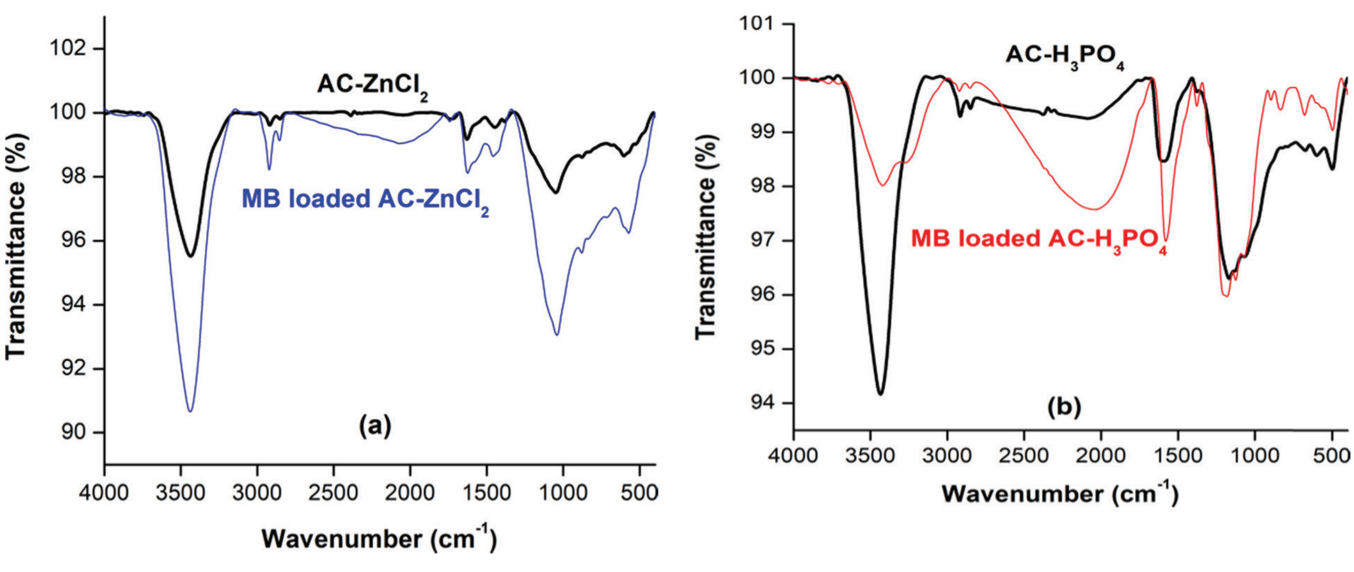

Figure 2: FTIR spectrum (a) AC-$ZnCl_2$ and (b) AC- H_3PO_4.

surface area. So, 350 mg/L and 200 mg/L are taken as the optimum dose for AC-$ZnCl_2$ and AC-H_3PO_4.

Isotherm Study

The Langmuir and Freundlich isotherm models were applied to the obtained adsorption capacity and various constants for adsorption of MB dye by using both ACs (Equations 3-4) are shown in Figure 4 and tabulated in Table 3. It can be seen that the adsorption capacity (q_m) of MB dye by AC-H_3PO_4 was found to be 213.21 mg/g which is higher than that of AC-$ZnCl_2$ (122.25 mg/g). Both the ACs show high value of correlation coefficient (R^2 =0.99) of Langmuir isotherm, however, uniform distribution activity and monolayer coverage were indicated onto the surface of AC-H_3PO_4. The R_L

Table 2: Functional Group in the IR Spectra of the activated carbon before and after MB adsorption (Lawrence, 2019)

Adsorption (cm^{-1})	*Functional group*	*Compound class*	*AC-$ZnCl_2$*	*AC- H_3PO_4*	*MB loaded AC-$ZnCl_2$*	*MB loaded AC- H_3PO_4*
3550-3200	O-H stretching	Alcohol	3436.39	3434.65	3441.88	3416.16
3000-2800	N-H stretching	amine salt (Strong)	2919.2	2927.3	2921.70	2928.63
2140-1990	N=C=S stretching	isothiocyanate	-	-	2067.85	2073.22
1670-1600	C=C stretching	Alkene	1638	1599.77	1619.23	-
1650-1580	N-H bending	Amine (medium)	-	-	-	1575.22
1600-1300	N-O stretching, C-H bending	nitro compound, alkane (methylene group)	-	-	1465.5	1371
1250-1020	C-N stretching, C-O stretching	Amine, Ester	-	1168.71	-	1174.73
1085-1050	C-O stretching	primary alcohol	1047.69	-	1047.23	-
1000-650	C=C, C-H bending	Alkene	-	-	888.97	842, 657.44

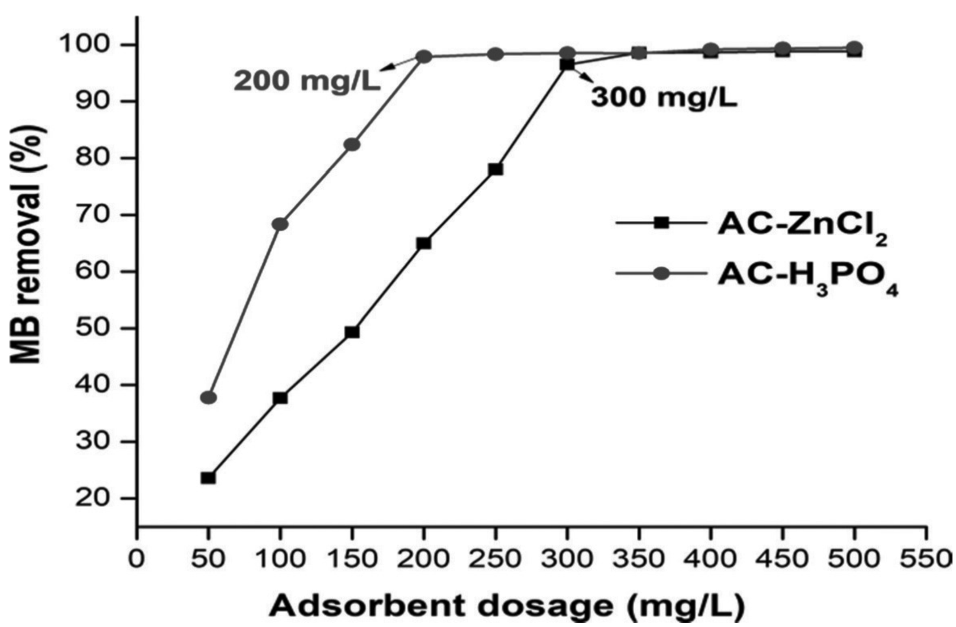

Figure 3: Effect of adsorption dosage on MB (C_o=25 mg/L, *T*= 30 ^oC).

(Equation 4) value shows whether the adsorption is (i) favourable (0 < R_L < 1) or unfavourable (R_L>1) (ii) linear (R_L=1) or irreversible (R_L= 0) (Khan et al., 2019). In the present work, the R_L value of both ACs was found to be 0<R_L<1; therefore, it confirms that the prepared AC from MS is favourable for the adsorption of MB dye. The parameters K_f and 1/n were also evaluated from the curve fitted to Freundlich adsorption isotherm as shown in Table 3. The correlation coefficient R^2 of both the AC is lower than the Langmuir isotherm, which means AC-$ZnCl_2$ and AC-H_3PO_4 do not closely follow the Freundlich isotherm.

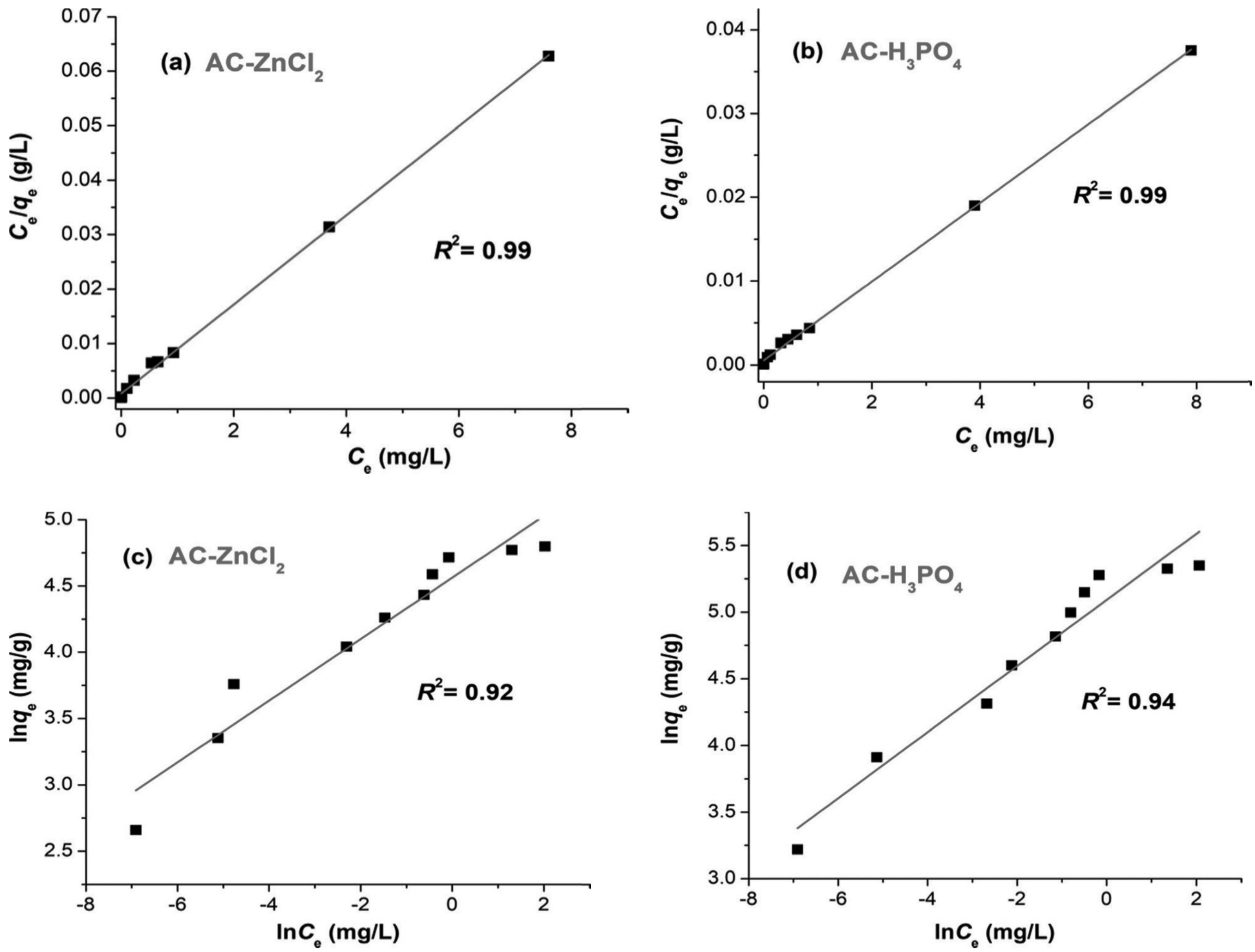

Figure 4: Linearised (a) and (b) Langmuir isotherm, and (c) and (d) Freundlich isotherm for MB adsorption by AC-$ZnCl_2$ (Dosage = 350 mg/L, T = 30 ºC) and AC-H_3PO_4 (pH = 8, Dosage = 200 mg/L, T = 30 ºC).

Table 3: Langmuir, Freundlich adsorption isotherm constant for MB dye on MSAC

AC	*Langmuir isotherm*				*Freundlich isotherm*		
	q_m (mg/g)	K (L/mg)	R^2	R_L	1/n	K_f (mg L/gm mg$^{1/n}$)	R^2
AC-$ZnCl_2$	122.25	9.77	0.99	0.0040	0.23	95.85	0.92
AC-H_3PO_4	213.21	8.40	0.99	0.0047	0.24	162.38	0.94

Discussion

The present study is based on the production of MS-based low-cost adsorbents using different activating agents. SEM and BET analyses confirm that the samples impregnated with $ZnCl_2$ and H_3PO_4 have a morphology similar to a honeycomb and significantly influenced the surface area and porosity of the activated carbon prepared from MS. Studies of FTIR spectra revealed that activating agents can alter functional surface groups from the MS. It is noticeable by the displacement and even the disappearance of some bands. This absence can be attributed to the loss of volatile compounds at 500 °C. Besides, there was a decrease in intensity of the bands, mainly around 3400 cm^{-1}, confirming the effects of activation in MS. Therefore, it is possible to verify that the produced activated carbon has chemical characteristics favourable for MB adsorption. These characteristics are closely related to the properties of the functional groups present on the surface of the adsorbent. In addition, its chemical balance was described by observing the Langmuir isotherm, suggesting chemical adsorption. Results indicate that activated carbon with $ZnCl_2$ and H_3PO_4 as activators presents an alternative adsorbent for the removal of MB. The comparison of theoretical adsorption capacities of MB using other biomass-based adsorbents obtained from isotherm models by different researchers is given in Table 4. In comparison, it is can be seen from the results of the present study that MSAC has sufficient adsorption capacities and BET surface area. Thus, MSAC is a green, low-cost adsorbent derived from an abundant and easily accessible agro waste material.

Table 4: Studies related to adsorption of MB dye using biomass-derived ACs

Biomass	*Activating agent*	*Experimental conditions (dose, temp. and rpm)*	*Adsorption capacity (mg/g)*	*BET surface area (m^2/g)*	*Isotherm model*	*References*
Rice husk	-	20 °C, 150 rpm	274.9	-	Freundlich	Alver et al., 2020
Coffee husk	KOH	1 g/L, 30 °C, 100 rpm	357.38	703.9	Langmuir	Tran et al., 2021
Mangosteen peels	H_3PO_4	-	871.49	1832	Langmuir	Zhang et al., 2021
Moringaoleifera leaf	NaOH	0.05g/L, 30 °C,	136.99	1.6881	Langmuir	Do et al., 2021
Banana pseudo-stem	-	0.2 g/L, 25 °C, 20 rpm	333.3	-	Freundlich	Bello et al., 2018
Mustard straw	$ZnCl_2$	0.35 g/L	122.25	402	Langmuir	In present study
Mustard straw	H_3PO_4	0.2 g/L	213.21	496	Langmuir	In present study

Conclusion

In the present study, AC was prepared from the mustard stalk by using $ZnCl_2$ and H_3PO_4 as activating agents for the adsorption of MB dye. The specific surface area of biochar was significantly increased by the activation using $ZnCl_2$ and H_3PO_4 and is found to be 402 and 496 m^2/g. The equilibrium data were suitably fitted by Langmuir isotherm over the Freundlich isotherm for both the AC. The adsorption capacity of AC-H_3PO_4 is 213.21 mg/g which is higher than that of AC-$ZnCl_2$ which is 122.25 mg/g due to the resultant high surface area available on adsorbent for removal of MB. This study showed that the AC prepared by chemical activation from MS biomass could be cost-effective, biofriendly and holds potential in various commercial applications.

Acknowledgements

The authors would like to thank the staff of Material Research Centre, Malaviya National Institute of Technology, Jaipur (Rajasthan), India for their kind support to make available analytical instruments. Also, financial help in the form of a project grant provided by Rajasthan Renewable Energy Corporation, Jaipur, India is highly acknowledged.

References

Alver, E., Metin, A.Ü. and F. Brouers (2020). Methylene blue adsorption on magnetic alginate/rice husk bio-composite. *International Journal of Biological Macromolecules*, **154:** 104-113.

Bello, K., Sarojini, B.K., Narayana, B., Rao, A. and K. Byrappa (2018). A study on adsorption behaviour of newly synthesized banana pseudo-stem derived superabsorbent hydrogels for cationic and anionic dye removal from effluents. *Carbohydrate Polymers*, **181:** 605-615.

Bulgariu, L., Escudero, L.B., Bello, O.S., Iqbal, M., Nisar, J., Adegoke, K.A., Alakhras, F., Kornaros, M. and I. Anastopoulos (2019). The utilization of leaf-based adsorbents for dyes removal: a review. *Journal of Molecular Liquid*, **276:** 728-747.

Do, T.H., Dung, N.Q., Chu, M.N., Van Kiet, D., Ngan, T.T.K. and L. Van Tan (2021). Study on methylene blue adsorption of activated carbon made from *Moringa oleifera* leaf. *Materials Today: Proceedings*, **38:** 3405-3413.

Fang, R. (2012). Preparation of corncob-based bio-char and its application in removing basic dyes from aqueous solution. *In: Advanced Materials Research*, **550:** 2420-2423 (Trans Tech Publications Ltd.).

Freundlich, H.M.F. (1906). Over the adsorption in solution. *Journal of Physical Chemistry*, **57(385471):** 1100-1107.

Gogoi, M.M., Babu, S.S., Moorthy, K.K., Bhuyan, P.K., Pathak, B., Subba, T., Chutia, L., Kundu, S.S., Bharali, C., Borgohain, A. and A. Guha (2017). Radiative effects of absorbing aerosols over northeastern India: Observations and model simulations. *Journal of Geophysical Research Atmosphere*, **122(2):** 1132-1152.

Gonzalez-Garcia, P. (2018). Activated carbon from lignocellulosics precursors: A review of the synthesis methods, characterization techniques and applications. *Renewable Sustainable Energy Review*, **82:** 1393-1414.

Hama, S.M., Kumar, P., Harrison, R.M., Bloss, W.J., Khare, M., Mishra, S., Namdeo, A., Sokhi, R., Goodman, P. and C. Sharma (2020). Four-year assessment of ambient particulate matter and trace gases in the Delhi-NCR region of India. *Sustainable Cities and Society*, **54:**102003

Jawad, A.H., Mehdi, Z.S., Ishak, M.A.M. and K. Ismail (2018). Large surface area activated carbon from low-rank coal via microwave-assisted KOH activation for methylene blue adsorption. *Dieselin Water Treat*, **110:** 239-249.

Khan, M.M.R., Sahoo, B., Mukherjee, A.K. and A. Naskar (2019). Biosorption of acid yellow-99 using mango (*Mangifera indica*) leaf powder, an economic agricultural waste. *SN Applied Sciences*, **1(11):** 1-15.

Langmuir, I. (1916). The constitution and fundamental properties of solids and liquids. Part I. Solids. *Journal of the American Chemical Society*, **38(11):** 2221-2295.

Lawrence, C.M. (2019). Organic Chemistry I Drill (CHEM2210D)-Module 2-Functional Groups and Infrared Spectroscopy.

Liu, B., Gu, J. and J.B. Zhou (2016). High surface area rice husk-based activated carbon prepared by chemical activation with $ZnCl_2$-$CuCl_2$ composite activator. *Environmental Progress and Sustainable Energy*, **35:** 133-140.

Liu, L., Ji, M. and F. Wang (2018). Adsorption of nitrate onto $ZnCl_2$-modified coconut granular activated carbon: kinetics, characteristics, and adsorption dynamics. *Advances in Materials Science and Engineering*, **2018:** 1939032.

Pandey, L.M. (2019). Enhanced adsorption capacity of designed bentonite and alginate beads for the effective removal of methylene blue. *Applied Clay Science*, **169:** 102-111.

Purohit, P. Tripathi, A.K. and T.C. Kandpal (2006). Energetics of coal substitution by briquettes of agricultural residues. *Energy*, **31:** 1321-1331.

Reffas, A., Bernardet, V., David, B., Reinert, L., Lehocine, M.B., Dubois, Batisse, N. and L. Duclaux (2010). Carbons prepared from coffee grounds by H_3PO_4 activation: Characterization and adsorption of methylene blue and Nylosan Red N-2RBL. *Journal of Hazardous Materials*, **175(1-3):** 779-788.

Sangon, S., Hunt, A.J., Attard, T.M., Mengchang, P., Ngernyen, Y. and N. Supanchaiyamat (2018).Valorisation of waste rice straw for the production of highly effective carbon based adsorbents for dyes removal. *Journal of Cleaner Production*, **172:** 1128-1139.

Siddiqui, S.I., Fatima, B., Tara, N., Rathi, G. and S.A. Chaudhry (2019). Recent advances in remediation of synthetic dyes from wastewaters using sustainable and low-cost adsorbents. *The impact and prospects of green chemistry for textile technology*, 471-507.

Singh, H., Sapra, P.K. and B.S. Sidhu (2013). Evaluation and characterization of different biomass residues through proximate & ultimate analysis and heating value. *Asian Journal of Engineering and Applied Technology*, **2(2):** 6-10.

Statista, https://www.statista.com/statistics/263930/worldwide-production-of-rapeseed-by- country (visited February 25, 2021)

Talaiekhozani, A., Mosayebi, M.R., Fulazzaky, M.A., Eskandari, Z. and R. Sanayee (2020). Combination of TiO_2 microreactor and electroflotation for organic pollutant removal from textile dyeing industry wastewater. *Alexandria Engineering Journal*, **59(2):** 549-563.

Tran, T.H., Le, H.H., Pham, T.H., Nguyen, D.T., La, D.D., Chang, S.W., Lee, S.M., Chung, W.J. and D.D. Nguyen (2021). Comparative study on methylene blue adsorption behaviour of coffee husk-derived activated carbon materials prepared using hydrothermal and soaking methods. *Journal of Environmental Chemical Engineering*, **9(4):** 105362.

Zhang, Z., Xu, L., Liu, Y., Feng, R., Zou, T., Zhang, Y., Kang, Y. and P. Zhou (2021). Efficient removal of methylene blue using the mesoporous activated carbon obtained from mangosteen peel wastes: Kinetic, equilibrium, and thermodynamic studies. *Microporous and Mesoporous Materials*, **315:**110904.